Nanotechnology Perceptions
ISSN 1660-6795
www.nano-*ntp.com*

"Formulation Evaluation And Development Of Manjistha Containing Anti-Pigmentation Hydrogel"

Md. Rageeb Md. Usman*[1], Gautam P. Vadnere[1], Neha R. Mali[1]

Department of Pharmacognosy
Smt. Sharadchandrika Suresh Patil College of Pharmacy, Chopda, Maharashtra, India.

This study explores the creation and assessment of a hydrogel enriched with Rubia cordifolia (commonly known as Manjistha) extract, valued for its anti-pigmentation and skin-brightening potential. A cornerstone of Ayurvedic medicine, Manjistha contains bioactive components like anthraquinones and glycosides, which contribute to its efficacy in regulating melanin production and providing antioxidant benefits. The hydrogel formulation was crafted using biocompatible and naturally derived polymers to ensure a pleasing texture and optimal application on the skin. Multiple formulations underwent evaluation for key physicochemical attributes, including pH balance, viscosity, spreadability, and stability. Emphasis was placed on achieving sustained release of active ingredients, enhancing skin absorption, and ensuring high compatibility with various skin types.

Keywords: Antioxidative Activity, Anthraquinones, Acrylic C10/30 Cross Polymer, Vacuum Distillation.

INTRODUCTION: Human skin shares similarities with the skin of many other mammals and closely resembles pig skin in structure. Despite being covered by hair follicles, most human skin appears hairless. Broadly, there are two types of skin: hairy and glabrous (hairless) skin. The term "cutaneous," derived from the Latin word cutis meaning skin, describes all things related to the skin. The skin serves as a crucial barrier, protecting the body from pathogens and preventing excessive water loss. Beyond this, it plays multiple roles, including insulating the body, regulating temperature, sensing external stimuli, synthesizing vitamin D, and safeguarding vitamin B folates. When severely damaged, skin undergoes a healing process, often resulting in the formation of scar tissue that can be discolored or depigmented. Human skin pigmentation is influenced by melanin, which is produced by melanocytes. [1] These cells, originating from mesodermal tissues, protect the body by absorbing harmful ultraviolet (UV) radiation. Additionally, skin contains DNA repair enzymes that help counteract UV-induced damage. Genetic deficiencies in these enzymes significantly increase susceptibility to skin cancer, particularly malignant melanoma—a highly invasive and potentially lethal form often caused by UV exposure. Skin pigmentation varies greatly among human populations, leading to classifications based on skin color. While the skin is the second-largest organ by surface area in the human body, following the small intestine's internal lining, it covers approximately 1.5–2.0 square meters (15–20 square feet) in an average adult. [2,3]

Hydrogel

A hydrogel is a biphasic material composed of a porous, permeable solid network and a substantial interstitial fluid, typically at least 10% by weight or volume, which is predominantly water. The solid component consists of a three-dimensional structure of natural or synthetic polymers that are water-insoluble, while the fluid allows the hydrogel to absorb significant amounts of water or biological fluids. [4] These characteristics make hydrogels particularly useful in various applications, especially in the biomedical field. While many hydrogels are synthetically produced, others are derived from natural sources. The term "hydrogel" was first introduced in 1894. These materials are part of a group of polymeric substances whose hydrophilic structure enables them to retain substantial water within their intricate networks. [5,6,7]

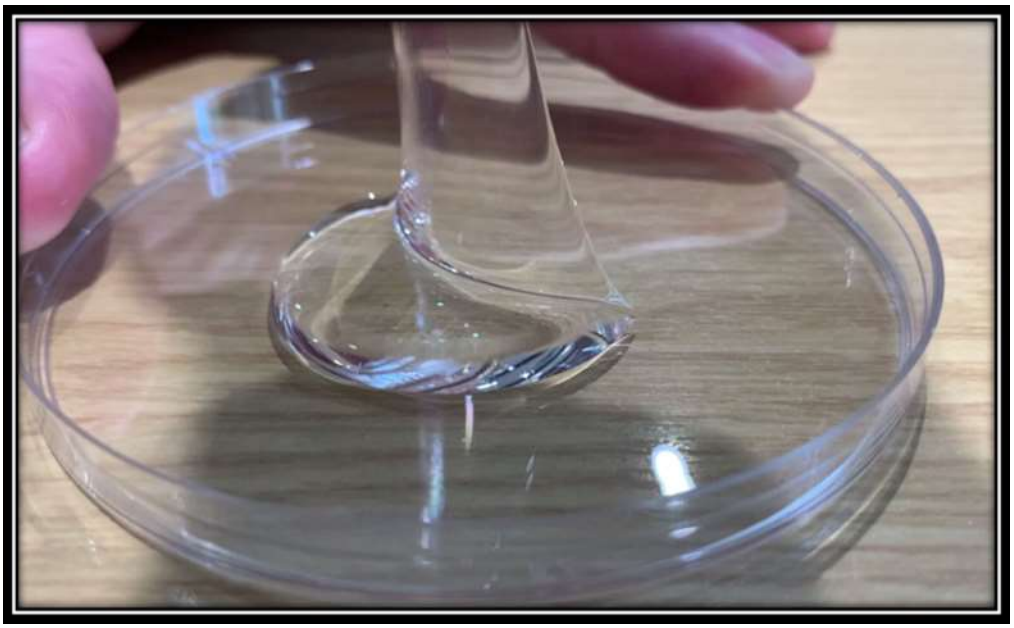

Fig.No.1: Hydrogel structure

Bases of Classification

1. Based on Source [7]
Hydrogels are divided into two main groups depending on their origin:

- **Natural Hydrogels**: Derived from natural sources.
- **Synthetic Hydrogels**: Created through artificial processes.

2. Based on Polymeric Composition [8]
The method of preparation results in various types of hydrogels:

- **Homopolymeric Hydrogels**: Composed of a polymer network derived from a single type of monomer, which serves as the basic building block.
- **Copolymeric Hydrogels**: Formed using two or more monomer species, at least one of which is hydrophilic. These monomers can be randomly arranged, alternating, or organized in blocks within the polymer chain.
- **Multipolymer Interpenetrating Hydrogels (IPNs)**: Consist of two independent cross-linked polymer networks, either synthetic or natural, interwoven in a single structure.

3. Based on Configuration [9]
Hydrogels can be classified based on their physical and chemical structures:

- **Amorphous**: Non-crystalline in nature.
- **Semicrystalline**: Contain a combination of amorphous and crystalline regions.
- **Crystalline**: Fully crystalline with an organized structure.

4. Based on Cross-Linking Type [10]
This classification considers the type of cross-links in the hydrogel network:

- **Chemically Cross-Linked Hydrogels**: Contain permanent cross-linking bonds.
- **Physically Cross-Linked Hydrogels**: Have transient junctions formed through interactions like ionic bonding, hydrogen bonding, or polymer chain entanglement.

5. Based on Physical Appearance [11,12]
The appearance of hydrogels depends on their preparation method and can vary as:

- Matrix
- Film
- Microsphere

6. Based on Electrical Charge in the Network [13]
Hydrogels are grouped according to the presence or absence of electrical charge in their cross-linked chains:

- **Nonionic**: Neutral with no electrical charge.
- **Ionic**: Include either anionic (negative) or cationic (positive) charges.
- **Amphoteric Electrolyte**: Contain both acidic and basic functional groups.
- **Zwitterionic**: Possess both anionic and cationic groups within each structural unit.

MATERIALS AND METHODS:

Methods:

Extraction Method: Vacuum distillation, performed at reduced pressures, offers a method for purifying compounds that are sensitive to ambient pressures or heat. By lowering the boiling point, this technique enables the separation of components based on their boiling point differences without risk of decomposition. [14,15] The boiling point reduction can be calculated using a temperature-pressure nomograph based on the Clausius–Clapeyron relation, ensuring precision and efficiency in compound extraction. [16]

Selection of base:
The main objective of the present study was to prepare an Anti-Pigmentation Hydrogel Formulation incorporated into the gel, hence gel base is used. [17,18]

Formulation of Anti-Pigmentation Hydrogel:

Table.1: Formulation Of Anti-Pigmentation Hydrogel

Ingredients	Parts Used	Category	Qty%
Manjistha	Roots	Anti-Pigmentation	5
EDTA	-	Chelating Agent	0.1
Trehalose 100	-	Moisturizing agent	0.1
Acrylicc10/30 Cross Polymer	-	Gelling agent	0.8
Glycerin	-	Humectant	5
Propanediol	-	Humectant	5
TEA	-	Neutralizer	0.3
Sodium Hyaluronate	-	Moisturizing Agent	0.2
Aristoflex	-	Gelling Agent	0.3
Ethylhexyl Glycerin	-	Preservative	0.8

Citric Acid	-	pH Stabilizer	0.1
Water	-	Solvent	82.3

EXPERIMENTAL WORK:

Extraction of Manjistha using Vacuum Distillation:
Vacuum Distillation

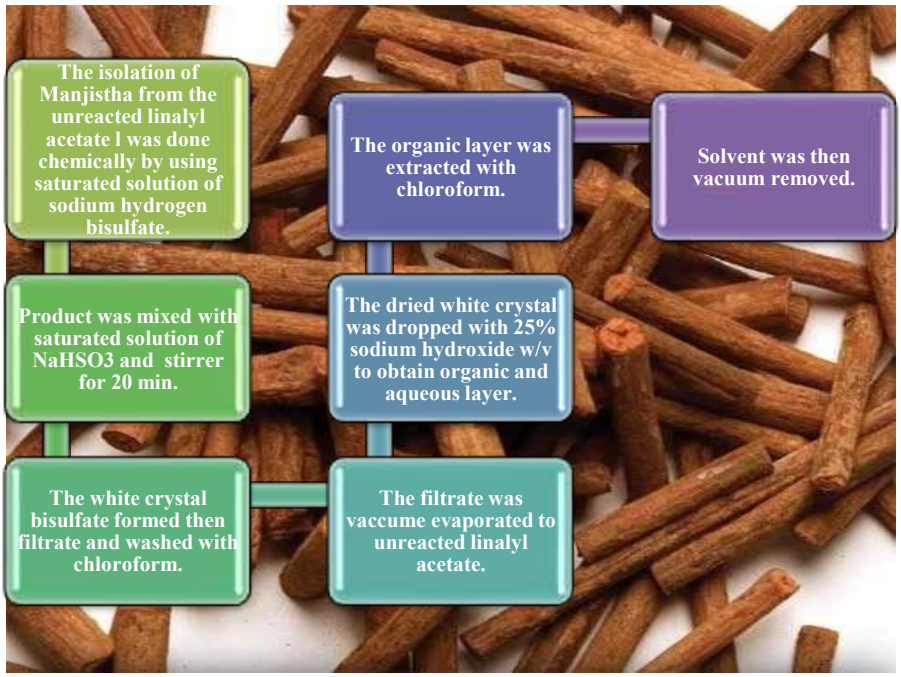

Fig No.2: Extraction of Manjistha Oil by Vacuum Distillation

Physical evaluation of Manjistha containing Anti-Pigmentation Hydrogel.

i) Fourier Transform Infrared Spectroscopy (FT-IR) FT-IR analysis was conducted to confirm the structural parameters of the formulations, including Manjistha oil, polymer, and the prepared hydrogel. Using the Perkin Elmer Spectrum RX-I FT-IR Spectrophotometer, the interaction between the drug and polymer was analyzed. Pellets were prepared with the KBr Disc method under 600 kg/cm² hydraulic pressure, and FT-IR spectra were scanned over a range of 3500–1000 cm^{-1} to record wave number values. [19]

ii) Thermal Analysis Thermogravimetric analysis (TGA) was performed on the optimized oil hydrogel. A 190 mg sample was placed in an aluminum pan, subjected to nitrogen gas flow at 20 ml/min, held at 40°C for 1 minute, and then heated from 40°C to 400°C at a rate of 10°C/min. The resulting thermogram was recorded using a PerkinElmer thermal analyzer. [20]

iii) Drug Release Study An in vitro drug release study was conducted using a USP Type-II dissolution apparatus. One gram of each hydrogel formulation was placed within a cellophane membrane and tied to the paddle. The release medium consisted of 500 ml PBS (pH 6.8) maintained at 37 ± 2°C, stirred at 100 RPM. Samples were taken at designated intervals, replaced with fresh PBS, and analyzed for absorbance at 290 nm using a UV spectrophotometer. Oil concentration in each formulation was calculated using a regression equation, and the study was performed in triplicate for accuracy. [21,22]

iv) Drug Release Kinetics Drug release patterns of the natural oil were evaluated using five kinetic models: zero-order, first-order, Higuchi, Hixson-Crowell, and Korsmeyer-Peppas. DD Solver (version 1.0) was utilized to determine the best-fit model, with Akaike Information Criterion (AIC) applied for model validity. [23,24]

v) Statistical Analysis Microsoft Excel (version 2013) was used to calculate statistical parameters, including mean and standard deviation. Regression analysis and ANOVA determined significant differences between the parameters of the 13 formulations, with $p < 0.05$ set as the significance threshold. [25,26]

vi) RSM Optimization Data Response Surface Methodology (RSM) was applied using polynomial equations with interaction and quadratic terms to optimize formulation variables. The % drug release in PBS (pH 6.8) over time was calculated using the Multiple Linear Regression Analysis (MLRA) approach. Contour plots and 3D graphs were generated to refine the formulation process for the desired output. [27]

vii) Determination of Sun Protection Factor (SPF) To determine SPF, 1 g of hydrogel was ultrasonicated in 100 ml ethanol for 10 minutes. After filtration, 5 ml of the aliquot was diluted to the mark in 50 ml volumetric flasks with ethanol, filtered again, and further diluted in 25 ml flasks. Using UV spectrophotometry, absorbance at 290–320 ± 5 nm was measured against ethanol as the reference. The SPF was calculated using established mathematical equations incorporating constants like the Erythemal Effect Spectrum (EE) and Correction Factor (CF = 10). [28]

viii) Antibacterial Activity Antibacterial evaluation was conducted using the Ditch plate technique with nutrient agar as the medium. Fresh pus from facial pimples was applied to agar plates using sterilized loops, and bacterial growth was observed after 24 hours at 25 ± 0.5°C. Optimized hydrogel (1 g) was applied to the agar plate, streaked, and incubated for another 24 hours. Microbial growth inhibition was assessed under a microscope using crystal violet dye. Inhibition length and % inhibition were calculated. [29,30]

RESULTS AND DISCUSSION

Vaccume Distillation

Result obtained by is shown in Table below

Table No 2: Weight of Oil With Respect To Time

Weight (g)	Time (mins)
0.35	250
0.40	500
0.50	750
0.55	100
0.65	1200

The oil produced by Vaccume Distillation Method is 2.45g weight of oil per 100g of dry leaves Fresh Lemongrass thereby producing 2.45% oil yield at 78^0C.

Table No 3: Result of Essential Oils Extraction

Method of extraction	% yield
vacuum Distillation	2.45

Calculation of Percentage Yield of Volatile Oil.

Material Balance for Vacuum Distillation Method

- Weight of Manjistha = 100g
- Quantity of hexane used= 600ml, Quantity of Ethanol used= 200ml
- Weight of beaker= 105.26g.
- Weight ethanol and essential oil= 202.55g.
- The weight of oil obtained= 2.45g.
- %yield = ME/MG x 100.
- Where, ME = Mass of essential oil MG = Mass of Manjistha sample
- ME = 2.45g MG = 100g.
- By substituting values.
- %yield = 2.45/100 x 100 =3.02%.
- Therefore % yield= 2.45%.

The graph below shows the plot of the weight of essential oil with respect to time for solvent extraction method.

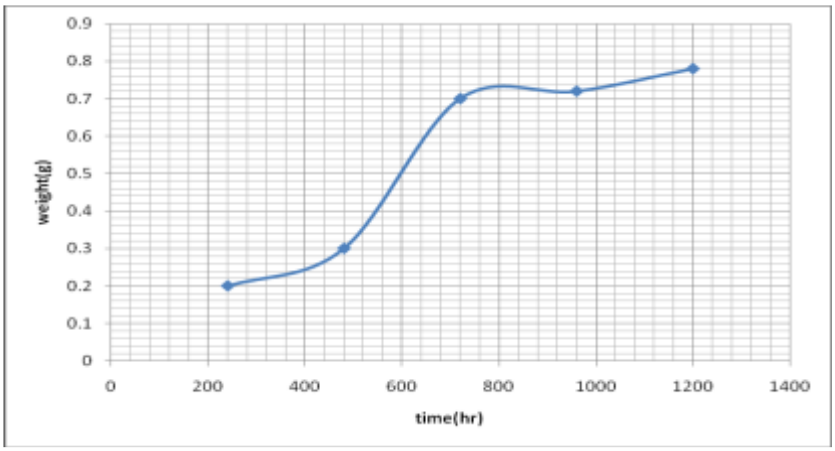

Fig. No. 3: Graph Below Shows the Plot of the Weight of Essential Oil with Respect to Time for Vacuum Distillation Method

Evaluation of Manjistha Oils Hydrogel formulations

i) Fourier Transform Infrared spectroscopy (FT- IR)

The FT-IR spectra analysis revealed no significant differences between the polymer (Acrylate Co-Polymer) and the optimized Manjistha oil hydrogel (EG6). Peaks observed in the range of 3000–3500 cm^{-1} were attributed to the alkane group ($-CH_3$). These peaks appeared sharper across all spectra, except for the polymer, likely due to the coordination of linkages. Peaks in the 1600–2395 cm^{-1} range corresponded to the alkene group (C=C), with sharper peaks in the polymer spectrum, indicating strong bond interactions within the polymer's alkene groups. Additionally, peaks in the range of 1020–1160 cm^{-1} suggested the presence of phenyl groups. The FT-IR results confirmed the stability of the oils within the hydrogel formulation. This stability was maintained in the presence of the Acrylate Co-Polymer and penetration enhancers, ensuring the consistency and integrity of the hydrogel.

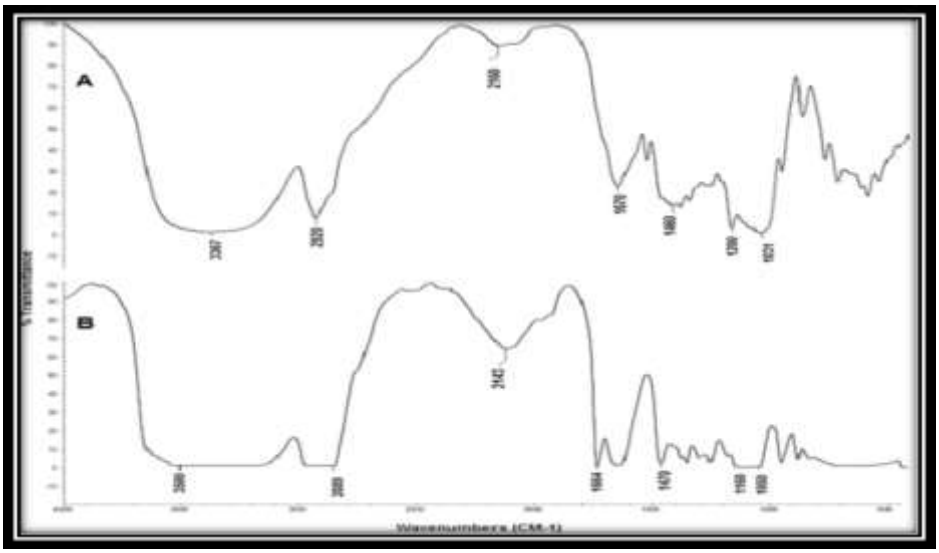

Fig.No.4: a) FTIR spectrum of extract b) FTIR Spectrum of Hydrogel formulation.

ii) Thermal analysis

The stability of oils within the Acrylate Co-Polymer matrix was assessed through thermal analysis using TGA thermograms. The melting point of the drug-loaded optimized EG6 hydrogel containing Manjistha oils was indicated by an exothermic single sharp peak at -23°C. The loading temperature during the process was maintained at 30°C. Results from the thermal analysis confirmed the molecular-level stability of the Manjistha oil hydrogel. The TGA curve for the optimized hydrogel further supported these findings.

iii) In vitro drug release study

The release of oils from all hydrogel formulations was assessed over a period of 24 hours. The release amount was calculated using a regression equation derived from the calibration curve: y = 0.0219 x

+ 0.1325 with regression coefficient R2 = 0.9994 at pH 6.8.

Results demonstrated that the EG4 hydrogel formulation exhibited the highest percentage of drug release, measured at 96.69% ± 0.01.The cumulative percentage drug release profiles for all hydrogel formulations at pH 6.8 (n=3 ± SD) were analyzed, revealing distinct patterns. The release profiles for formulations EG1, EG2, and EG13 showed an abrupt release of oils, primarily attributable to their high release rates under the given conditions.

iv) Drug release kinetics

The mode of drug release for the formulated Manjistha oil hydrogels was determined to follow the Korsmeyer-Peppas model. This model was identified as the most suitable for the hydrogels at pH 5.5, as it demonstrated the highest coefficient of determination ($R2$) and the lowest Akaike Information Criterion (AIC) value compared to other models, as presented in Table 6. These findings indicate that the drug release mechanism is independent of the drug concentration. Furthermore, the hydrogel formulations exhibited Fickian diffusion, as the diffusion exponent (n) was less than 0.45.

Table No 4: Drug release

Time min	EG1 (%)	EG2 (%)	EG3 (%)	EG4(%)
0	13.58 ±0.01	13.35 ±0.01	14.04 ±0.01	10.4± 0.1

5	19.75 ±0.01	18.61 ±0.01	19.06 ±0.01	19.75 ±0.01
10	23.4± 0.01	24.1± 0.1	23.86 ±0.01	24.54 ±0.01
15	27.73 ±0.01	28.88 ±0.01	29.57 ±0.01	29.56 ±0.01
30	32.99 ±0.01	34.8± 0.1	35.27 ±0.01	35.04 ±0.01
45	37.10 ±0.01	41.44 ±0.01	40.98 ±0.01	40.75 ±0.01
60	41.66 ±0.01	46.9± 0.1	47.37 ±0.01	48.51 ±0.01
90	46.46 ±0.01	56.1± 0.1	56.74 ±0.01	57.19 ±0.01
120	56.50 ±0.01	60.01 ±0.01	61.07 ±0.01	62.67 ±0.01
150	62.67 ±0.01	67.69 ±0.01	67.24 ±0.01	69.52 ±0.01
180	69.29 ±0.01	73.85 ±0.01	74.32 ±0.01	74.54 ±0.01
240	78.19 ±0.01	79.3± 0.1	80.25 ±0.01	78.88 ±0.01
300	83.67 ±0.01	82.3± 0.1	83.45 ±0.01	81.4± 0.1
360	87.10 ±0.01	84.8± 0.1	86.19 ±0.01	84.13 ±0.01
1440	93.26 ±0.01	90.98 ±0.01	91.67 ±0.01	90.52 ±0.01

v) RSM Optimization data modeling

Multiple linear regression analysis was used to establish a mathematical relationship, expressed through a polynomial equation. A positive coefficient value indicated a synergistic effect, whereas a negative value suggested an antagonistic effect on the response. A larger coefficient value highlighted the factor's stronger impact on the response. The analysis results showed a percentage coefficient of variation (17.33%), F-value (3.72), $R2$=0.75, and mean ± SD (86.29 ± 14.95).

vi) Effect of enhancers on % drug release at Y (pH 5.5)

The significance probability P-value (p>0.05) for response Y indicated that linear participation produced a non-significant synergistic effect (p<0.05). In contrast, cross-product participation also resulted in a non-significant antagonistic effect (p<0.05). Quadratic contribution $A2$ exhibited a significant (p>0.05) antagonistic effect, whereas $B2$ showed a non-significant (p<0.05) antagonistic effect. The polynomial equation, in terms of coded factors, is as follows:

Y= 96.75+38.28A +26.35B -20.79AB – 30.68 A2-4.07 B2

vii) Optimization of Manjistha Oils Hydrogel formulations

Drug release profiles from different oil hydrogel formulations through cellophane membranes were compared over a 24-hour period. Results derived from RSM data analysis, contour plots, and 3D surface plots showed that the EG4 hydrogel formulation had the highest drug release (96.69%) at pH 6.8 compared to other formulations. EG4 demonstrated faster release through the cellophane membrane and maximum drug release, leading to its selection as the optimized formulation for further ex-vivo and in-vivo studies in animal/human models.

viii) Determination of Sun Protection Factor (SPF)

SPF values of up to 20 are considered ideal for skin protection. The SPF values of all oil hydrogel formulations ranged from 14.56 ± 0.01 to 19.9 ± 0.01, demonstrating their effectiveness in protecting against ultraviolet rays. The optimized formulation exhibited an SPF value consistent with previous findings, confirming its suitability for skin protection.

ix) Antibacterial activity

The optimized EG4 hydrogel exhibited 85% inhibition, confirming its antibacterial efficacy against microbial activity on the skin. This strong antibacterial and antimicrobial activity makes the formulation safe for transdermal use. Similar findings from previous studies support the effectiveness of herbal oils. Manjistha oil, rich in polyunsaturated fatty acids like alpha-linoleic acid, is known to reduce inflammation. Additionally, its analgesic and anti-inflammatory properties, attributed to the presence of vitamin C, make the hydrogel potentially useful for treating rheumatoid arthritis and other inflammatory conditions, as supported by literature

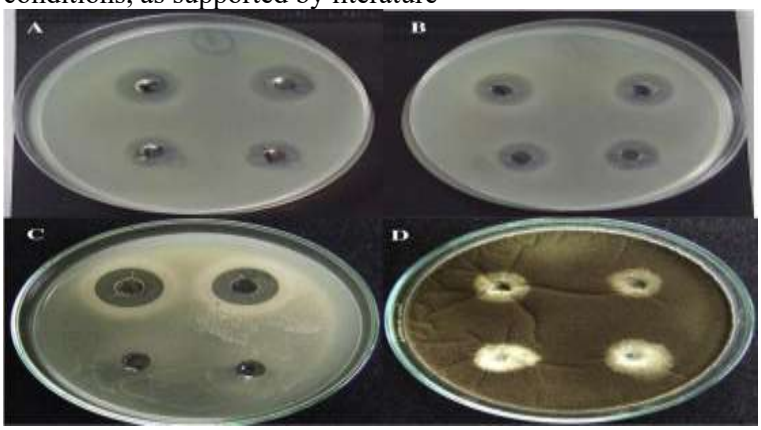

Fig.No. 5: Antibacterial activity

CONCLUSION:

The study on the formulation, evaluation, and development of Manjistha-containing anti-pigmentation hydrogel concluded that the prepared formulation was highly effective. The hydrogel, incorporating Rubia cordifolia (Manjistha), demonstrated significant cooling properties along with antibacterial, anti-inflammatory, and antioxidant effects. The formulation exhibited a semi-solid consistency with excellent homogeneity and ease of application, enhancing its overall usability.

In summary, the Manjistha-containing hydrogel emerged as a promising and viable solution for treating hyperpigmentation and improving skin health.

Vacuum distillation methods were highlighted as efficient and effective techniques for extracting essential oils for applications such as shower gels. This method remains one of the most commonly utilized and economically viable approaches for essential oil extraction in the modern herbal industry, primarily due to its simplicity and reliability.

ACKNOWLEDGEMENT: The authors are thankful to the Principal, Smt. Sharadchandrika Suresh Patil College of Pharmacy, Chopda, Maharashtra, India. necessary facilities for research work.

CONFLICTS OF INTEREST: Authors have no conflicts of interest to declare.

REFERENCES:

1. Afrin S., Gupta V. Pharmaceutical Formulation. StatPearls Publishing; Treasure Island, FL, USA: 2020.

2. Sharma S., Singh S. Dermatological preparations, formulation and evaluation of various semi-solid dosage form. Asian J. Pharm. Res. Dev. 2014;2:10–25.

3. Sharadha M., Gowda D., Gupta V., Akhila A. An overview on topical drug delivery system–updated review. Int. J. Res. Pharm. Sci. 2020;11:368–385. doi: 10.26452/ijrps.v11i1.1831.

4. Yu Y.-Q., Yang X., Wu X.-F., Fan Y.-B. Enhancing Permeation of Drug Molecules Across the Skin via Delivery in Nanocarriers: Novel Strategies for Effective Transdermal Applications. Front. Bioeng. Biotechnol. 2021;9:646554. doi: 10.3389/fbioe.2021.646554.

5. Choi H., Kwon M., Choi H.E., Hahn S.K., Kim K.S. Non-Invasive Topical Drug-Delivery System Using Hyaluronate Nanogels Crosslinked via Click Chemistry. Materials. 2021;14:1504. doi: 10.3390/ma14061504.

6. Badola A., Goyal M., Baluni S. Gels And Jellies A Recent Technology In Semisolids: A. World J. Pharm. Res. 2021;10:461–475.

7. Jeganath S., Jeevitha E. Pharmaceutical Gels and Recent Trends-A Review. Res. J. Pharm. Technol. 2019;12:6181–6186.

8. Zielińska A., Eder P., Rannier L., Cardoso J.C., Severino P., Silva A.M., Souto E.B. Hydrogels for modified-release drug delivery systems. Curr. Pharm. Des. 2021 doi: 10.2174/1381612828666211230114755.

9. Bustamante-Torres M., Romero-Fierro D., Arcentales-Vera B., Palomino K., Magaña H., Bucio E. Hydrogels Classification According to the Physical or Chemical Interactions and as Stimuli-Sensitive Materials. Gels. 2021;7:182. doi: 10.3390/gels7040182.

10. Voci S., Gagliardi A., Molinaro R., Fresta M., Cosco D. Recent Advances of Taxol-Loaded Biocompatible Nanocarriers Embedded in Natural Polymer-Based Hydrogels. Gels. 2021;7:33. doi: 10.3390/gels7020033.

11. Alven S., Aderibigbe B.A. Chitosan and Cellulose-Based Hydrogels for Wound Management. Int. J. Mol. Sci. 2020;21:9656. doi: 10.3390/ijms21249656.

12. Michalik R., Wandzik I. A mini-review on chitosan-based hydrogels with potential for sustainable agricultural applications. Polymers. 2020;12:2425. doi: 10.3390/polym12102425.

13. Cai M.-H., Chen X.-Y., Fu L.-Q., Du W.-L., Yang X., Mou X.-Z., Hu P.-Y. Design and development of hybrid hydrogels for biomedical applications: Recent trends in anticancer drug delivery and tissue engineering. Front. Bioeng. Biotechnol. 2021;9 doi: 10.3389/fbioe.2021.630943.

14. Russo E., Villa C. Poloxamer hydrogels for biomedical applications. Pharmaceutics. 2019;11:671. doi: 10.3390/pharmaceutics11120671.

15. .Patel K.D., Silva L.B., Park Y., Shakouri T., Keskin-Erdogan Z., Sawadkar P., Cho K.J., Knowles J.C., Chau D.Y., Kim H.-W. Recent advances in drug delivery systems for glaucoma treatment. Mater. Today Nano. 2022:100178. doi: 10.1016/j.mtnano.2022.100178. [DOI] [Google Scholar]

16. Veloso S.R., Andrade R.G., Castanheira E.M. Review on the advancements of magnetic gels: Towards multifunctional magnetic liposome-hydrogel composites for biomedical applications. Adv. Colloid Interface Sci. 2021;288:102351. doi: 10.1016/j.cis.2020.102351.

17. Gallo E., Diaferia C., Rosa E., Smaldone G., Morelli G., Accardo A. Peptide-Based Hydrogels and Nanogels for Delivery of Doxorubicin. Int. J. Nanomed. 2021;16:1617. doi: 10.2147/IJN.S296272.

18. Gonzalez-Delgado J.A., Castro P.M., Machado A., Araujo F., Rodrigues F., Korsak B., Ferreira M., Tome J.P., Sarmento B. Hydrogels containing porphyrin-loaded nanoparticles for topical photodynamic applications. Int. J. Pharm. 2016;510:221–231. doi: 10.1016/j.ijpharm.2016.06.037.

19. Jøraholmen M.W., Johannessen M., Gravningen K., Puolakkainen M., Acharya G., Basnet P., Škalko-Basnet N. Liposomes-In-Hydrogel Delivery System Enhances the Potential of Resveratrol in Combating Vaginal Chlamydia Infection. Pharmaceutics. 2020;12:1203. doi: 10.3390/pharmaceutics12121203.

20. Marafon P., Fachel F.N.S., Dal Prá M., Bassani V.L., Koester L.S., Henriques A.T., Braganhol E., Teixeira H.F. Development, physico-chemical characterization and in-vitro studies of hydrogels containing rosmarinic acid-loaded nanoemulsion for topical application. J. Pharm. Pharmacol. 2019;71:1199–1208. doi: 10.1111/jphp.13102.

21. Kelmann R.G., Colombo M., Nunes R.J., Simões C.M., Koester L.S. Nanoemulsion-loaded hydrogels for topical administration of pentyl gallate. Aaps Pharmscitech. 2018;19:2672–2678. doi: 10.1208/s12249-018-1099-8.

22. Cardoso A.M., de Oliveira E.G., Coradini K., Bruinsmann F.A., Aguirre T., Lorenzoni R., Barcelos R.C.S., Roversi K., Rossato D.R., Pohlmann A.R. Chitosan hydrogels containing nanoencapsulated phenytoin for cutaneous use: Skin permeation/penetration and efficacy in wound healing. Mater. Sci. Eng. C. 2019;96:205–217. doi: 10.1016/j.msec.2018.11.013.

23. Wei S., Xie J., Luo Y., Ma Y., Tang S., Yue P., Yang M. Hyaluronic acid based nanocrystals hydrogels for enhanced topical delivery of drug: A case study. Carbohydr. Polym. 2018;202:64–71. doi: 10.1016/j.carbpol.2018.08.112.

24. Furlani F., Rossi A., Grimaudo M.A., Bassi G., Giusto E., Molinari F., Lista F., Montesi M., Panseri S. Controlled Liposome Delivery from Chitosan-Based Thermosensitive Hydrogel for Regenerative Medicine. Int. J. Mol. Sci. 2022;23:894. doi: 10.3390/ijms23020894.

25. Rashid S.A., Bashir S., Naseem F., Farid A., Rather I.A., Hakeem K.R. Olive Oil Based Methotrexate Loaded Topical Nanoemulsion Gel for the Treatment of Imiquimod Induced Psoriasis-like Skin Inflammation in an Animal Model. Biology. 2021;10:1121. doi: 10.3390/biology10111121.

26. Hung W.-H., Chen P.-K., Fang C.-W., Lin Y.-C., Wu P.-C. Preparation and Evaluation of Azelaic Acid Topical Microemulsion Formulation: In Vitro and In Vivo Study. Pharmaceutics. 2021;13:410. doi: 10.3390/pharmaceutics13030410.

27. Khan S., Jain P., Jain S., Jain R., Bhargava S., Jain A. Topical delivery of erythromycin through cubosomes for acne. Pharm. Nanotechnol. 2018;6:38–47. doi: 10.2174/2211738506666180209100222.

28. Sharma P., Dhawan S., Nanda S. Cubosome: A Potential Liquid Crystalline Carrier System. Curr. Pharm. Des. 2020;26:3300–3316.

29. Kaur S.D., Singh G., Singh G., Singhal K., Kant S., Bedi N. Cubosomes as Potential Nanocarrier for Drug Delivery: A Comprehensive Review. J. Pharm. Res. Int. 2021;33:118–135. doi: 10.9734/jpri/2021/v33i31B31698.

30. Im S.H., Jung H.T., Ho M.J., Lee J.E., Kim H.T., Kim D.Y., Lee H.C., Choi Y.S., Kang M.J. Montelukast nanocrystals for transdermal delivery with improved chemical stability. Pharmaceutics. 2020;12:18.